Grating amplitude effect on electroluminescence enhancement of corrugated organic light-emitting devices

Xu-Lin Zhang,[1] Jing Feng,[1,3] Jun-Feng Song,[1,2] Xian-Bin Li,[1] and Hong-Bo Sun[1,4]

[1]*State Key Laboratory on Integrated Optoelectronics, College of Electronic Science and Engineering, Jilin University, 2699 Qianjin Street, Changchun 130012, China*

[2]*Institute of Microelectronics, A*STAR (Agency for Science, Technology and Research), 11 Science Park Road, Singapore Science Park II, Singapore 117685*

[3]*e-mail: jingfeng@jlu.edu.cn*

[4]*e-mail: hbsun@jlu.edu.cn*

Received July 28, 2011; revised August 29, 2011; accepted September 3, 2011; posted September 7, 2011 (Doc. ID 151923); published September 30, 2011

We report grating amplitude dependence of electroluminescence (EL) in organic light-emitting devices with one-dimensional corrugated structure. Our proposed devices can emit light from both the top silver and bottom quartz side, and both exhibit amplitude-dependence EL enhancement. The effect of grating amplitude on the EL intensity has been studied experimentally and numerically to find out the optimal grating amplitude for the greatest EL enhancement. We deduce from the numerical simulations and experimental results that surface plasmon-polariton modes and waveguide modes are coupled out of the corrugated devices efficiently at the optimal amplitude; therefore, higher efficiency of light extraction could be realized.

OCIS codes: 050.1950, 310.6845.

It has been reported that up to 40% of the light produced in a typical planar organic light-emitting device (OLED) based on small molecules may be lost to SPP modes, and can be recovered by introducing an appropriate periodic corrugation onto the cathode surface [1–6]. Surface plasmon polariton (SPP)-mediated emission from an OLED incorporating a periodic wavelength scale corrugation has been observed [7–13], and the coupling through waveguide (WG) modes or Fabry–Perot (FP) modes can also attribute to the light extraction. When the periodic grating is introduced, besides the grating period, the grating amplitude is an important factor to affect the coupling efficiency. However, less attention has been paid to the grating amplitude effect.

In this Letter, a detailed experimental and numerical study of the grating amplitude effect on the emission efficiency of corrugated OLEDs is performed. By introducing one-dimensional (1D) corrugation, the EL intensity both from the top silver side and the bottom quartz side of the OLEDs is obviously enhanced. Optimal grating amplitude is determined to obtain the greatest EL intensity.

A 1D corrugation is introduced into a quartz substrate by a holographic lithography technique [12,14,15]. The corrugated quartz substrate is coated with a 150 nm thick indium-tin-oxide (ITO) layer as the anode by dc magnetron sputtering. Three layers are then vacuum deposited to form the device: 100 nm thick N,N'-diphenyl-N,N'-bis(1-naphthyl)-(1,1'-biphenyl)-4,4'-diamine (NPB) as the hole-transporting material, 80 nm thick tris-(8-hydroxyquinoline)aluminum (Alq_3) as the emitting material, and 50 nm thick silver layer as the cathode (Fig. 1). Although a rough metal-dielectric surface may also support SPP, a grating structure with period of 550 nm is chosen in this work, which enables the control of the SPP peaks close to the emitting peak of Alq_3 to enhance the light extraction. Five OLEDs are fabricated with grating amplitude h [see Fig. 1(a)] of 15 nm, 30 nm, 50 nm, 70 nm, and 85 nm, respectively, to examine the amplitude effect. For comparison, an uncorrugated device is fabricated on the planar region of the same quartz substrate, side by side with the corrugated device, which is also shown in Fig. 1(a). The emitting area for all the devices is 2 mm in diameter.

To measure the performance of our devices, the samples are placed on a rotation stage with the grooves parallel to the rotation axis. An aperture is used to limit the angular acceptance to ~1°. The drive voltage we apply to obtain the spectra for all flat and corrugated devices is 12 V.

The p-polarized emission spectra at $\theta = 0°$ from the silver and quartz sides with different amplitudes are shown in Figs. 2(a) and 2(b), respectively. The same trends of EL from both the silver and quartz sides are observed that the EL intensity first increases until it reaches its maximum at $h = 70$ nm and then decreases with further increase of the amplitude. The emission spectra of the silver side with different emission angles are illustrated in Fig. 2(c), from which splitting of the original peak into two peaks can be observed with increase of θ. This is the characterization of the SPP or WG mode. Since the SPP

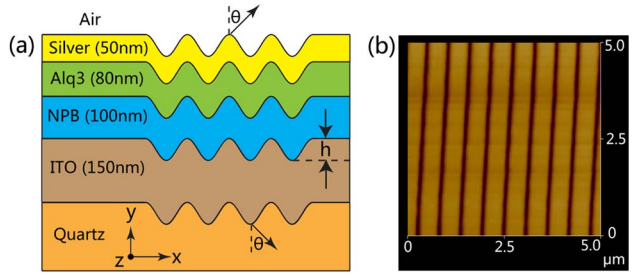

Fig. 1. (Color online) (a) Configuration of the corrugated and flat OLEDs side by side. (b) Atomic-force microscope image of the 1D corrugated quartz substrate with 550 nm as the grating period.

has not much effect on the spontaneous emission of materials with high quantum efficiency [16,17], such as Alq_3 (~30%), the grating effect is mainly on improving the external efficiency by outcoupling of the trapped optical modes.

We apply our in-house generated finite-difference time-domain (FDTD) codes to analyze the origins of the peaks in Fig. 2. The main purpose of the simulation is to verify the enhancement induced by the SPP or WG mode in the EL spectra. The Drude model is chosen to deal with silver. The refractive indices of other materials (e.g., NPB) employed in OLEDs are measured by ellipsometry experimentally for the FDTD calculation. Period boundary conditions and perfectly matched layers are set along the x direction and y direction, respectively. The incident light is a modulated Gaussian pulse centered at 600 nm. The reflection, transmission, and absorption spectra can be obtained by Fourier transform. The spontaneous emission process in the Alq_3 layer is quite complicated, which is difficult to be modeled by the FDTD method directly. Here, instead of directly simulating the EL spectra, we set the incidence opposite to the EL direction in order to excite the same modes in our OLEDs. Then as the SPP (WG) mode can help enhance the absorption, our simulated absorption spectra may have the same peaks as the EL spectra, and this is the main idea of our simulations.

The simulated p-polarized absorption spectra from both the silver and quartz sides at $\theta = 0°$ with different grating amplitudes are given in Figs. 3(a) and 3(b), respectively. The peak wavelengths are basically consistent with those in Figs. 2(a) and 2(b), while the negligible differences are attributed to the fabrication size variations and the FDTD calculation errors. Note that the spectra shape between the calculated absorption and measured EL emission is different. This is because the emission spectrum of the Alq_3 layer is not taken into consideration in the simulation. To investigate the mode profiles of the three peaks in Figs. 3(a) and 3(b), we calculate the steady-state H_z field intensity distribution of the transverse magnetic (TM) mode with $h = 70$ nm and the results are given in Figs. 3(c)–3(e), corresponding to the fields (c)–(e) in Figs. 3(a) and 3(b) with wavelength of 590 nm, 595 nm, and 510 nm, respectively. It is obvious from Fig. 3(c) that at a wavelength of 590 nm, coupling to the SPP mode at the Ag/Air interface is obtained together with the enhanced light extraction from the silver side. Meanwhile, from Figs. 3(d) and 3(e), at wavelengths of 595 nm and 510 nm, light can be coupled out of the quartz side more efficiently due to the coupling out of the SPP mode at the Ag/Alq_3 interface and the WG mode in the ITO layer, respectively. Moreover, as is illustrated by the black curve in Fig. 3(b), the peak of our flat OLED is attributed to the FP effect in the ITO layer, with its H_z field intensity of the TM mode drawn in Fig. 3(f). The SPP and WG peak positions mainly decided by the grating period are close to the peak emission of Alq_3 (about 520 nm) in order to enhance the EL intensity.

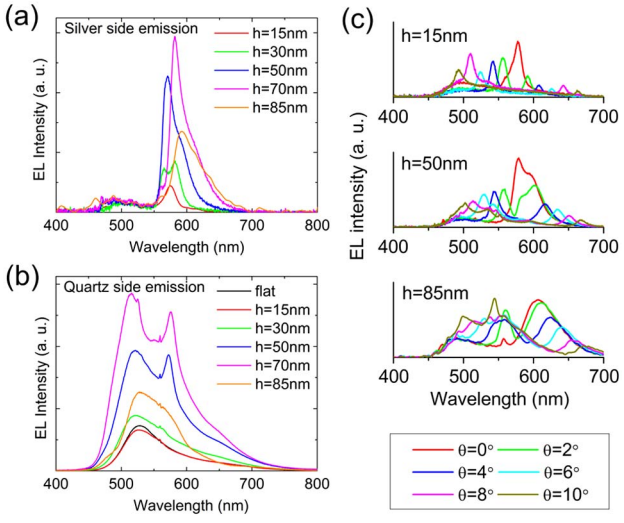

Fig. 2. (Color online) (a),(b) EL spectra observed at normal directions with different grating amplitudes from (a) silver side and (b) quartz side, respectively. (c) Angular dependence of EL spectra observed from the silver side with different grating amplitudes.

Now we can discuss more thoroughly about the grating amplitude effect. The trends of absorption intensity with respect to the grating amplitude in the silver side [Fig. 3(a)] and the quartz side [Fig. 3(b)] are different: the intensity of the SPP mode at the Ag/Air interface increases with the amplitude until it reaches its maximum at $h = 70$ nm, which coincides with the experimental observation of the silver side. For the quartz side, the intensity of the related SPP mode at the Ag/Alq_3 interface and WG mode in the ITO layer both increase with the amplitude but without going through its maximum, which is not consistent with the present experiment. In our

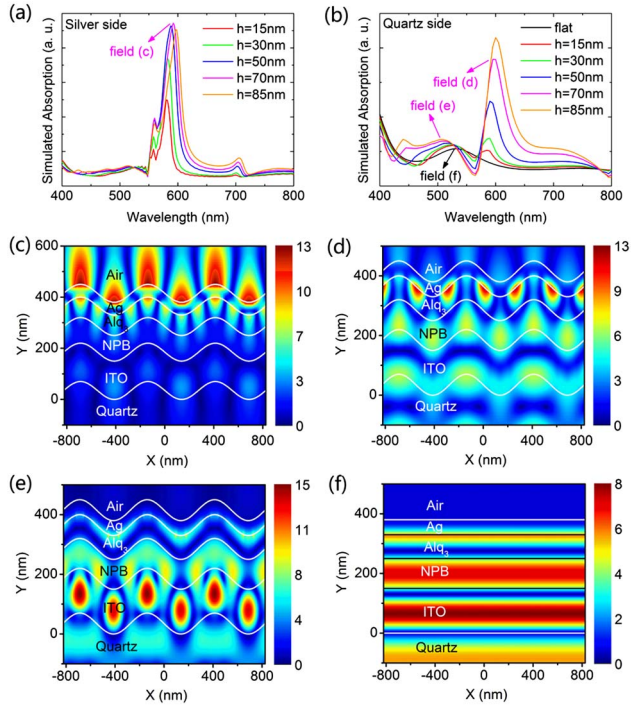

Fig. 3. (Color online) (a),(b) FDTD simulated absorption with p-polarized incidence at normal directions from (a) silver side and (b) quartz side with different grating amplitudes. (c)–(f) FDTD simulated steady-state H_z field intensity distribution of TM mode at normal direction with $h = 70$ nm, where the wavelengths are (c) 590 nm from silver side, (d) 595 nm from quartz side, (e) 510 nm from quartz side, and (f) 530 nm from quartz side but without grating.

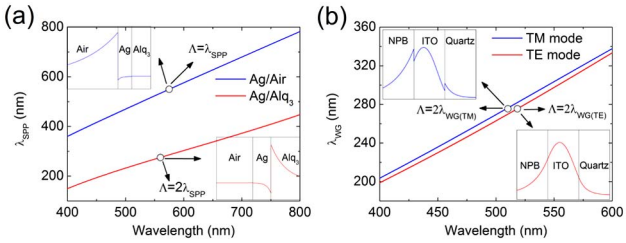

Fig. 4. (Color online) Effective SPP (WG) wavelength with respect to the wavelength of the (a) SPP modes at Ag/Air and Ag/Alq_3 interfaces, respectively, and (b) both TM and TE WG modes supported by the ITO layer. The white circles indicate the wavelengths that satisfy Eq. (1) with their S_x fields drawn in the insets.

opinion, the greatest EL intensity corresponds to the strongest coupling of the light emitted from the Alq_3 layer to the SPP (WG) mode. However, with increased grating amplitude (higher than 70 nm in our experiment), the thickness variations for the following deposited electrode and organic functional layers would be increased, which may cause nonuniform current flow across the OLED materials and result in a degradation of the OLED performance. A redshift of SPP peak with increasing amplitude can be found, which is due to the increase of wavelength of the SPP mode because of surface corrugation. Based on the above discussion, the optimal grating amplitude is confirmed to be 70 nm, at which improved external efficiency by outcoupling of optical modes into free space is obtained.

Then we discuss the grating diffraction orders of the SPP (WG) mode to sustain our FDTD simulation. The condition of the coupling SPP (WG) mode to radiation mode in 1D grating OLEDs can be described by:

$$\Lambda = m\lambda_{\mathrm{SPP(WG)}}, \tag{1}$$

where $\lambda_{\mathrm{SPP(WG)}}$ is the effective SPP (WG) wavelength, which equals to λ/n_{eff}, n_{eff} is the effective refractive index of the SPP (WG) mode, Λ is the grating period, and m is the grating diffraction order. The above equation is only applied for $\theta = 0°$. The physical sense of Eq. (1) is that one period of periodic relief should contain integer number of SPP (WG) wavelengths. The optical waveguide theory and transfer matrix method are applied to calculate the effective SPP (WG) wavelength. The main procedure is to solve the scalar Helmholtz equation and then apply the related boundary condition to get the total transfer matrix.

The simulation results are shown in Figs. 4(a) and 4(b), where the effective SPP (WG) wavelength is calculated with respect to the wavelength. In Fig. 4(a), the blue and red curves represent the effective SPP wavelength of TM modes at the Ag/Air and Ag/Alq_3 interfaces, respectively, which increases with the increasing wavelength. So with a fixed m, there should be only one wavelength that satisfies Eq. (1). The wavelengths that meet the conditions at the Ag/Air and Ag/Alq_3 interfaces are marked by two white circles, corresponding to the first-order and second-order grating diffractions, respectively. Notice that the wavelengths obtained by the FDTD method and optical waveguide theory are close to each other, which supports the validity of both our calculations. The x direction normalized energy flows-S_x component fields are given in the insets of Fig. 4(a), from which the SPP modes supported by the Ag/Air and Ag/Alq_3 interfaces can be clearly seen. Figure 4(b) plots the effective WG wavelength of both TM and TE modes supported by the ITO layer. The two marked white circles represent that the WG modes arise by the second-order grating diffractions, and insets for their S_x fields. From the above mode analysis, our FDTD results are confirmed.

In summary, we have obtained enhanced EL from both top and bottom sides of the OLEDs with 1D corrugated structures. The grating amplitude effect is thoroughly studied and the optimal grating amplitude of 70 nm in experiment is determined to obtain the greatest EL intensity. The origins of the enhancement are found to be in relation with the excitation and coupling out of the SPP and WG modes via the FDTD method and optical waveguide theory. Since the optimal amplitude can help enhance the light absorption, it may find application as well in other types of optoelectronic devices, such as solar cells.

The authors gratefully acknowledge support from the "973" Project under grant 2011CB013005, and from the National Natural Science Foundation of China (NSFC) (grants 60977025, 90923037, and 61177024).

References

1. R. H. Raether, *Surface Plasmons on Smooth and Rough Surfaces and on Gratings* (Springer, 1988).
2. W. C. Liu and D. P. Tsai, Phys. Rev. B **65**, 155423 (2002).
3. T. W. Ebbesen, H. J. Lezec, H. F. Ghaemi, T. Thio, and P. A. Wolff, Nature **391**, 667 (1998).
4. T. Thio, H. F. Ghaemi, H. J. Lezec, P. A. Wolff, and T. W. Ebbesen, J. Opt. Soc. Am. B **16**, 1743 (1999).
5. H. F. Ghaemi, T. Thio, D. E. Grupp, T. W. Ebbesen, and H. J. Lezec, Phys. Rev. B **58**, 6779 (1998).
6. P. A. Hobson, S. Wedge, J. A. E. Wasey, I. Sage, and W. L. Barnes, Adv. Mater. **14**, 1393 (2002).
7. C. J. Yates, I. D. W. Samuel, P. L. Burn, S. Wedge, and W. L. Barnes, Appl. Phys. Lett. **88**, 161105 (2006).
8. J. M. Lupton, B. J. Matterson, I. D. W. Samuel, M. J. Jory, and W. L. Barnes, Appl. Phys. Lett. **77**, 3340 (2000).
9. S. Wedge, I. R. Hooper, I. Sage, and W. L. Barns, Phys. Rev. B **69**, 245418 (2004).
10. Y. Liu and S. Blair, Opt. Express **12**, 3686 (2004).
11. D. K. Gifford and D. G. Hall, Appl. Phys. Lett. **81**, 4315 (2002).
12. J. Feng, T. Okamoto, and S. Kawata, Opt. Lett. **30**, 2302 (2005).
13. S. R. J. Brueck, V. Diadiuk, T. Jones, and W. Lenth, Appl. Phys. Lett. **46**, 915 (1985).
14. J. Feng, T. Okamoto, and S. Kawata, Appl. Phys. Lett. **87**, 241109 (2005).
15. J. Feng, T. Okamoto, R. Naraoka, and S. Kawata, Appl. Phys. Lett. **93**, 051106 (2008).
16. G. Sun, J. B. Khurgin, and R. A. Soref, Appl. Phys. Lett. **90**, 111107 (2007).
17. J. B. Khurgin, G. Sun, and R. A. Soref, J. Opt. Soc. Am. B **24**, 1968 (2007).